Bioelectrochemistry 74 (2008) 83–89

Contents lists available at ScienceDirect

Bioelectrochemistry

journal homepage: www.elsevier.com/locate/bioelechem

Direct electrochemical study of the multiple redox centers of hydrogenase from *Desulfovibrio gigas*

Cristina M. Cordas, Isabel Moura, José J.G. Moura *

REQUIMTE - Departamento de Química, CQFB, Faculdade de Ciências e Tecnologia, Universidade Nova de Lisboa, 2859-516 Monte de Caparica, Portugal

ARTICLE INFO

Article history:
Received 30 May 2007
Received in revised form 10 April 2008
Accepted 12 April 2008
Available online 26 April 2008

Keywords:
Hydrogenases
Biocatalysis
Electrochemistry
Activation

ABSTRACT

Direct electrochemical response was first time observed for the redox centers of *Desulfovibrio gigas* [NiFe]-Hase, in non-turnover conditions, by cyclic voltammetry, in solution at glassy carbon electrode. The activation of the enzyme was achieved by reduction with H_2 and by electrochemical control and electrocatalytic activity was observed. The inactivation of the [NiFe]-Hase was also attained through potential control. All electrochemical data was obtained in the absence of enzyme inhibitors. The results are discussed in the context of the proposed mechanism currently accepted for activation/inactivation of [NiFe]-Hases.

1. Introduction

Hydrogenases (Hases) are multicenter enzymes that catalyse the interconversion between H_2 and H^+, involved in the sulphate respiration pathway, by which anaerobic organisms get energy, using hydrogen as an electron donor. Hase is responsible for the hydrogen metabolism, according to the bidirectional reaction $H_2 \leftrightharpoons 2H^+ + 2e$. In sulphate reducing bacteria the sulphate reduction occurs on the cytoplasm and the hydrogen oxidation on the periplasm, and so, the electron transport is accomplished by redox complexes involving multiheme cytochromes, with emphasis to cytochrome c_3, that seems to be the preferential physiological partner [1]. The importance of Hase enzymes is due to its great technological interest for the H_2 production, either through the use of the whole cells or the isolated enzymes, the use in biofuel cells, as biosensors, for its possible role on the biocorrosion mechanisms and also in possible applications in decontamination of environments [2,3].

There are three different classes of hydrogenases that are classified based on the metals present in the catalytic center, namely nickel–iron [NiFe] (a variant is the [NiFeSe] enzymes), iron–iron [FeFe] and non-iron (metal-free hydrogenase) that in fact was recently proved to contain Fe and CO [4,5]. The [NiFe]-Hase from *Desulfovibrio gigas* (*Dg*) is a periplasmic enzyme with molecular weight of 89 kDa formed by two subunits (with 26 and 63 kDa), in which the larger contains the active site and the smaller one holds three iron–sulfur clusters, namely one [3Fe-4S] and two [4Fe-4S] [6]. It is currently accepted that these clusters function as the electronic pathway to transfer electrons to the [NiFe] center. The active sites of the different [NiFe]-Hases present high structural similarity. The metal center presents one Fe atom bond to one CO and two CN ligands, which is an unusual coordination in biology [7]. Ni is coordinated by four cysteines, two of which form a bridge to the Fe atom. The oxidized form of the protein presents another ligand in bridge configuration between the Ni and the Fe atoms. The nature and role of this extra ligand has been extensively discussed. It is well established that this is an oxygenated specie, but the exact form depends on the catalytic site activation state and is still under discussion [8,9]. [NiFe]-Hase presents several redox states that correspond to active and inactive forms of the enzyme. So far at least seven different redox states have been identified to be related with the possible electron and proton transfers and ligand bonds [4,10]. In the inactive oxidised enzyme two states are described, the so-called Ni–A "unready" and the Ni–B "ready" species, both EPR detectable, with Ni signals of S=1/2, and present in the as-isolated protein [6]. These two forms differ on the required activation time, with Ni–B being much faster (in a manner of minutes) while Ni–A requires long time (several hours) under H_2 to be active. EPR, ^{17}O ENDOR and crystallographic data suggest that the bridge ligand on Ni–A is a diatomic ligand like O_2^- [11] while on Ni–B seems to be a monoatomic oxygen species, also compatible with a hydroxide [9,12]. Ni–A and Ni–B can be further reduced to form EPR silent states, namely Ni–SU (unready) and Ni–SI (two forms, ready and active) and the Ni–C, the so-called "active" form, and Ni–R states (fully reduced form), these last two EPR detectable species [8,9]. A very simplified scheme showing the main states Ni–A, Ni–B, Ni–C and the silent ready and active states is shown in Fig. 1. The previous active enzyme was proved to become inactive by oxidation with O_2, in agreement with

* Corresponding author. Tel.: +351 21 2948382; fax: +351 21 2948550.
E-mail address: jose.moura@dq.fct.unl.pt (J.J.G. Moura).

1567-5394/$ – see front matter © 2008 Elsevier B.V. All rights reserved.
doi:10.1016/j.bioelechem.2008.04.019

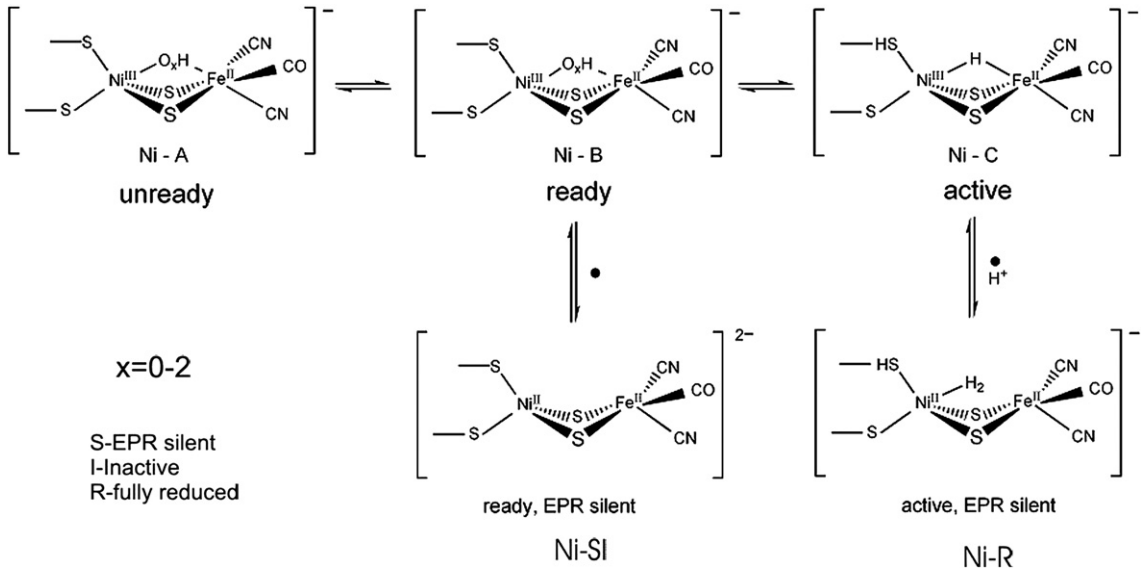

Fig. 1. Simplified scheme showing the main Hase states, namely Ni–A, Ni–B, Ni–C and the silent ready and active-fully reduced states (SI and R). The stoichiometry of the oxygenated specie that binds to the Ni–Fe center is still under discussion.

the hypothesis that the oxygenated species bond hinders the H_2 capture [13].

The discussion remains about the Ni oxidation state during the catalytic cycle, with the hypothesis of Ni(III), Ni(II) or even Ni(I) involvement [4]. Although the catalytic mechanism is still under discussion, one model for the reaction is described as the H_2 fixation to the Ni(II) at the Ni–SI form, heterolytic cleavage to form a protonated intermediate, that may be a bridge hydride between the Ni and the Fe atoms, assigned as the Ni–C form [14]. Follows the subsequent production of the reduced state Ni–R and re-oxidation with regeneration of the Ni–SI, passing by the Ni–C form [15]. Another pertinent discovery is the presence of a gas channel localized from the protein surface towards the Ni atom, giving support to the idea that Ni has the main role on the catalysis mechanism [16]. The proposed catalytic mechanisms, based on theoretical calculations, for the above reaction are quite complex, and involve two cycles whether if it is the H_2 production or consumption and if the control is electrochemical or by reduction under hydrogen [4].

Electrochemical techniques are important tools to understand enzyme mechanisms and the intrinsic electrocatalytic properties and different approaches are possible such as immobilization by adsorption like protein film voltammetry [13,17], or by the use of membranes [18], modified electrodes [19], or in solution [15].

Several studies of the electrocatalytic activity of different hydrogenases have been performed, where the rate of H_2 production and consumption is studied, either with systems where the Hase is immobilized [13] or using in bulk mediators, such as methyl viologen [15,20]. Although these studies have been important to enlighten the catalytic mechanism, the redox signals of the individual metallic centers were not clearly observed. Armstrong and co-workers were able to observe some redox features besides the catalytic activity for Hase isolated from *Chromatium vinosum* with the enzyme adsorbed on a rotating pyrolytic graphite disk electrode. These authors have applied CO which inhibited the catalytic activity of the enzyme allowing the observation of two redox peaks [21].

In the present work we were able to observe, for the first time, without using any inhibitors, the electrochemical response of [NiFe]-Hase redox centers, in non-turnover conditions, tuned by electrochemical control. *Dg* Hase direct electrochemical behaviour was studied, by cyclic voltammetry, in solution at glassy carbon electrode. Direct electron exchange between the electrode and the enzyme was successful. The activation of the enzyme was achieved by H_2 reduction and by electrochemical control and electrocatalytic activity was observed. Inactivation of [NiFe]-Hase was also attained through potential control, by cyclic voltammetry.

2. Experimental

2.1. Purification

All purification procedures were performed at 4 °C starting from a *Dg* cell-free crude extract. A more straightforward purification scheme involving less steps and using DEAE-52, Superdex 75 and HTP columns was introduced in order to improve the purification of hydrogenase described before [22]. Purity was verified by electrophoresis and visible spectroscopy (purity ratio A_{400}/A_{280}=0.27). The EPR patterns obtained (not shown) confirm that the protein was purified in the Ni–A state.

2.2. Electrochemical studies

The potentiodynamic measurements were performed with a Potenciostat/Galvanostat AUTOLAB PGSTAT 12. One compartment electrochemical cell was used. Glassy carbon (GC) and pyrolytic graphite (PG) were used as working electrodes with diameters of 3 and 4 mm, respectively. The counter electrode was a Pt wire and the reference was a saturated calomel electrode (SCE). The potential values in the text are reported in the normal hydrogen electrode (NHE) reference. The working electrodes were previously treated by immersion in concentrated nitric acid and polished with alumina with different grades, then immersed in Millipore water in an ultra-sound bath and finally thoroughly rinsed with Millipore water. The experiments were performed with the protein in bulk solution with concentrations 1–3 μM. The electrolyte composition was 25 mM Tris–HCl, Acetate, CHES or Phosphate buffer/0.1 M NaCl/1 mM neomicyn sulfate. The cyclic voltammetry (CV) was performed at different scan rates (from 2.5 mV/s to 2 V/s).

3. Results and discussion

3.1. Activation under H_2

Electrochemical experiments with *Dg* [NiFe]-Hase was attained with the protein in bulk solution (Fig. 2). It was possible to observe the direct electrochemical response of the *Dg* Hase either using the GC or the PG electrode. The cyclic voltammograms, in anaerobic conditions (anaerobic chamber, <20 ppm O_2), with a dilute 2 μM solution,

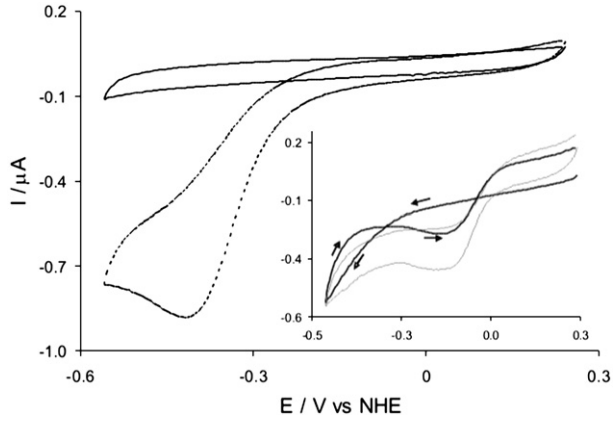

Fig. 2. Cyclic voltammograms of a dilute 2 µM Hase solution (black dashed line) in an anaerobic chamber (<20 ppm O_2), ν=50 mV/s, at GC electrode, after previous activation with H_2 by overnight incubation at 4 °C, at pH 7, and control obtained without Hase (black solid line). Inset: the same conditions after repetitive cycling followed by a resting period at the open circuit potential (1st scan black line, subsequent scans grey line).

obtained after previous activation with H_2 by overnight incubation at 4 °C, at pH 7, (ν=50 mV/s) show a reduction peak at approximately −0.40 V, corresponding to the reduction of protons and the formation of H_2. After multiple cycles and a resting period at open circuit potential until its stabilization, the electrochemical pattern changes and the subsequent cycles show two current crossings resulting from the fact that the reverse scan present lower current than the forward one (in the scanning cathodic direction). The first current crossing occurs at the potential value of −0.278 V, previous to the development of a cathodic current wave, with a maximum around −0.108 V, and the second crossing point at −0.027 V. The cathodic peak due to the H^+ reduction reaction, is observed at a considerably higher potential value (−0.108 V) than in the first assay performed with the enzyme activated by H_2 incubation. The initial forward scan does not present any cathodic peak. The potential at which the cathodic peak is observed on the reverse scan and the current crossings are indicative of the lower energy necessary to promote the hydrogen reduction reaction. The observed current crossings, are probably due to the formation of a hydride [23,24] bond between the nickel and iron atoms of the active protein site. After the observation of these current crossings, the subsequent scans present the characteristic shape of the catalytic current peak, in which the current starts to develop at −0.008 V in contrast with the higher potential value observed immediately after the chemical activation of Hase. The difference in the observed potential values at which the catalytic current develops between the first cycle where the Hase was activated by H_2 incubation only and in the later potential sweeps in which the protein has been already subjected to multiple potential cycles may be indicative of the lower energy needed to release the H_2 produced in the later case. This fact seems coherent with an "electrochemical activation" of the enzyme. The lower energy requirement for the reduction of H^+ (or $H^{\cdot}$) may be related to a mechanism intermediate, in this case a hydride, and we may be observing the H+/H• production from the break of the hydride bridge with the Ni atom.

The H^+/H_2 potential variation suggest that we are observing two different mechanisms by which the reaction occurs on Hase. This is in agreement with previous suggestions, based on density functional theory (DFT), that two different pathways are possible whether the potential control is made by imposing a H_2 pressure and reduction or if it is imposed electrochemically [4]. In the mentioned proposed mechanism the electrochemical controlled catalytic cycle predicts a very fast Ni(I) intermediate. This last assumption is not absolutely clear from the electrochemical data obtained at pH 7.6, although a small reduction wave observed at a more negative potential value of −0.408 V may be related with this reduced Ni form. This signal is better seen at lower pH (later on the text).

Another set of experiments was performed to study the scan rate variation effect on the catalytic current peak. The protein incubated with H_2 was subjected to multiple scans, with different scan rates (2.5 mV/s to 2 V/s), but, contrarily to the former assays, without a resting period. The resulting voltammograms (Fig. 3) show a clear variation in the catalytic response pattern, that change from a typical catalytic sigmoidal curve for the smaller scan rates to a broad wave, characteristic of a diffusion controlled process. It was not possible, however, to completely eliminate the catalytic reaction even with the maximum scan rate applied (2 V/s) due to the high turnover of this enzyme [17,25]. It should be noted that the maximum of the catalytic current peak is observed at lower potential values than the obtained for the same conditions, before the imposed resting period, shown before, suggesting that the multiple potential cycling has electrochemically activated the enzyme.

3.2. Redox centers response

The same experimental conditions were tried but with no previous activation step of the enzyme. The enzyme was purified in aerobic conditions and it was kept that way previous to the electrochemical assay. In these conditions, it was possible to observe the direct electrochemical response of the metallic centers of the [NiFe]-Hase by cyclic voltammetry (Fig. 4). Three redox processes can be identified, namely the cathodic process designated by I, around −0.36 V, process II at −0.258 V with the anodic counterpart at −0.098 V and the well defined redox couple, III, at −0.078 V and 0.008 V, respectively the cathodic and anodic peaks. A comparison with the literature values obtained by electrochemical techniques and by EPR and Mössbauer

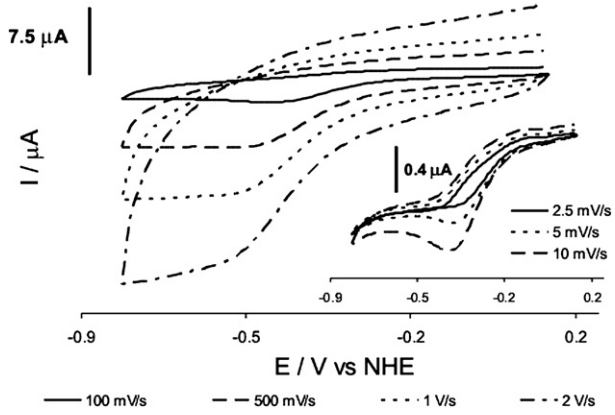

Fig. 3. Cyclic voltammogram of the *Dg* Hase in a dilute solution (3 µM), obtained in anaerobic conditions, at pH 7, with different scan rates from 2.5 mV/s to 2 V/s at the PG electrode. In the figure are plotted the first scans of each scan rate.

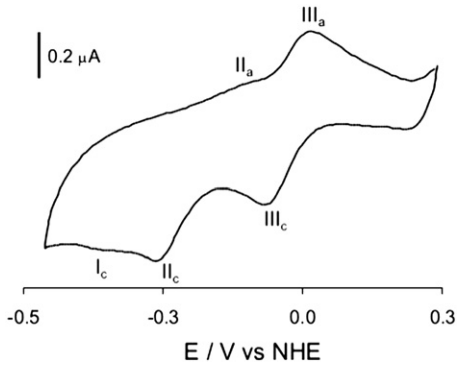

Fig. 4. Cyclic voltammogram of the *Dg* Hase in a dilute solution (3 µM), obtained in anaerobic conditions, at pH 7, ν=50 mV/s, using the GC electrode. The voltammogram is the result from the blank subtraction for better observation of the redox processes of the enzyme.

spectroscopies together with a closer look to the structure of the enzyme was done in order to assign the observed redox processes [6,21,26]. Processes I and II were attributed to the $[4Fe\text{-}4S]_{dist}$ cluster and Ni (III/II), respectively. The well defined process III may be due to the [3Fe-4S] cluster because of its higher potential value [21,27,28]. Although the [3Fe-4S] clusters can undergo to one or two electron processes, from our data and considering an approximation to a reversible process in bulk, the number of estimated electrons associated with the redox process III was 0.90±0.13, so we have concluded that this cluster undergoes a one electron transfer reaction. So the difference in size between the different centers must be attributed to its possible different accessibility and electron transfer kinetics. The estimated midpoint potential, E°' was −0.032 V.

Reduction of the protein at −0.558 V during different times followed by the potential scan in the anodic direction (−0.558 to 0.242 V) results in the observation of a new anodic wave, I_a around −0.36 V, and to a better definition of process II_a at −0.088 V, related with the cathodic processes designated by I_c and II_c showing the reversibility of the processes (Fig. 5). A new sharp anodic peak appears at −0.258 V that should be due to the oxidation of the hydrogen produced at −0.558 V [25]. This phenomenon arises because the long reduction time probably implies the accumulation of an amount of adsorbed molecules to the electrode surface large enough to allow its oxidation to be detectable in the time scale of the technique.

This was the first time, to our knowledge, that these redox centers were observed in non-turnover conditions and without the use of any enzyme inhibitor.

3.3. Electrochemical activation

The same experimental conditions as in the previous assays, with the protein in bulk solution, were again tried, with no previous activation of the enzyme. Next experiments were again performed on strict anaerobic conditions (anaerobic chamber). The electrochemical activation of the Hase was achieved by multiple cycling between +0.192 and −0.958 V at low scan rate (5 mV/s). The cyclic voltammograms obtained show again current crossings, around −0.558 V, simultaneously with some hydrogen evolution reaction. It should be noted (see inset of Fig. 6A) that a cathodic wave develops, on the first cycle, on the forward scan, around −0.22 V. The reverse scan, after the current crossing, shows a smaller anodic wave at −0.058 V. These cross-cuttings may be related with the adsorption of Hydrogen on the Ni–Fe center during the process of the hydrogen fixation and/or hydride formation [24]. Other hypothesis to explain the current cross-cuttings are related with changes in the enzyme/electrode interface, namely adsorption/desorption processes of the Hase on the glassy carbon. However, assays where the electrode, after being subjected to multiple scans in the presence of Hase, was removed rinsed with Millipore water and then immersed in the same electrolyte but in the absence of Hase, did not revealed any electrochemical features that could be related with adsorption of Hase. For this reason, in our experimental conditions, the cross-cuttings were attributed to changes in the Hase centers. Despite these results a deeper surface analysis should help to elucidate this point and it is planned in future work.

After cycling, a resting period at the open circuit potential was imposed, after which the same potential window was tested. The result was a typical catalytic current, showing that the electrochemical activation of the Hase was well succeeded. The catalytic waves midpoint potential for the enzyme activated o/n in a hydrogen atmosphere (Fig. 2) and for the Hase electrochemically activated are different, namely in the first case −0.051 V and in the second −0.281 V. This may result from the activation/catalysis mechanism that may be different in the two cases.

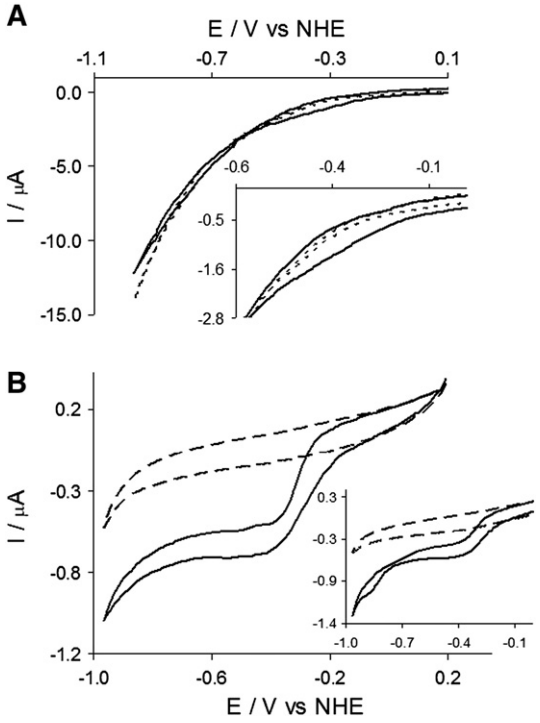

Fig. 6. Cyclic voltammogram of the *Dg* Hase in a dilute solution (3 μM), obtained in anaerobic conditions, ν=5 mV/s at pH 4.5 and at the GC electrode; A) 1st (solid line) and 3rd cycles (dashed line), inset: larger view of the potential window 0 to −0.6 V and B) after electrochemical activation with multiple scanning and a resting period (45 min) at the open potential (solid line) and the control assay (dashed line), inset: the same experiment at pH 5 (solid line) and the control assay (dashed line); it is possible to see the extra redox process assigned to Ni (II)/(I) (arrow).

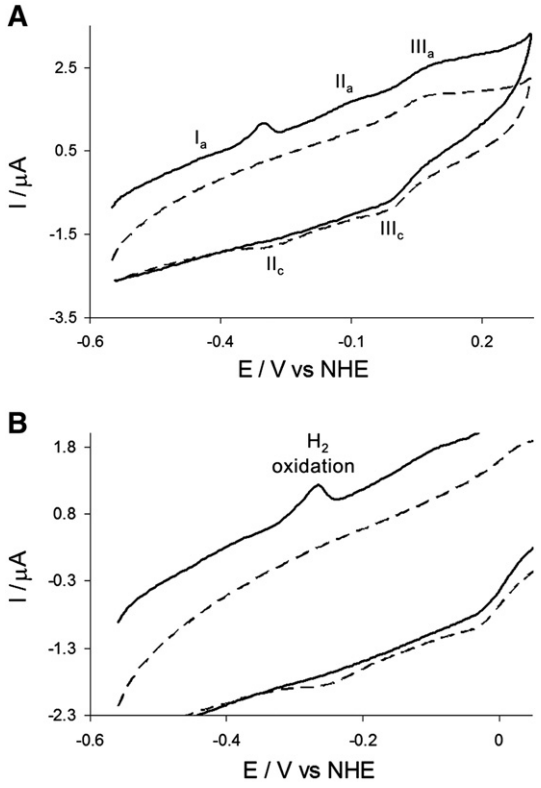

Fig. 5. Cyclic voltammograms of the *Dg* Hase in a dilute solution (3 μM), obtained in anaerobic conditions, at pH 7, ν=100 mV/s, at the GC electrode; the potential was kept at −0.558 V previous to the scan in the anodic direction for 0 s (dashed line) and 600 s (solid line), A) full range window and B) amplification to clearer observation of the H_2 oxidation signal.

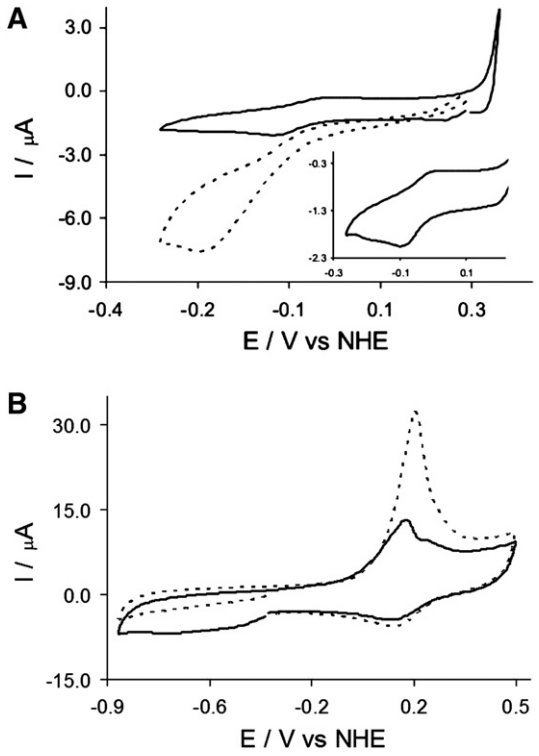

Fig. 7. Cyclic voltammogram of the *Dg* Hase in a dilute solution (2 μM), in anaerobic conditions, ν=50 mV/s, pH 7.6, at the PG electrode; A) 1st (dashed line) and 2nd (solid line) scans in a wider anodic potential range and B) after inactivation in a wider potential range, 1st (dashed line) and 2nd (solid line) scans.

The Hase electrochemical activation was tested at different pH values. Besides the catalytic current, the subsequent voltammogram after the electrochemical activation, obtained at pH 5 or below, display another redox process at a more negative potential (see inset of Fig. 6B). This cathodic wave after the catalytic process is probably due to a second reduction of the Ni atom, probably from Ni(II) to NI(I). This is in agreement with published data, namely potential values obtained by redox titrations [21], together with EPR experiments and theoretical calculations that point to the existence of a possible two electron reduction that would remove the hydride and generate a Ni(I) specie [29]. Some studies have proven the existence of a paramagnetic Ni–L state that is obtained from the reduction of Ni–C upon illumination and at cryogenic temperatures. This was proved to be a reversible reaction that reverts to Ni–C with the temperature increase. DFT calculations showed that this state is related with the loss of a proton from the bridging position between Ni and Fe atoms resulting in a formal oxidation state Ni(I) that seems in good agreement with the g-values obtained experimentally [30]. In our assays, the driving force energy obtained at low potential values such as the imposed to the system at which the signal attributed to the Ni(II)/Ni(I) redox couple is observed, namely −0.86 V, is probably enough to achieve this state. The Hase electrochemical activation was only possible to achieve in strict anaerobic conditions. Outside the anaerobic chamber, even with highly degassed solutions with an argon flux, it was not possible to accomplish this potential modelling activation. This is probably due to the high sensibility to oxygen presented by the *Dg* [NiFe]-Hase [31] and the role of the non-active forms of the enzyme with oxo/hydroxo bridge species between the Ni and Fe atoms.

3.4. Electrochemical inactivation

Another set of experiments was made with *Dg* [NiFe]-Hase in bulk, in which a different potential window was tried, again in strict anaerobic conditions and pH 7.6. The goal was to inactivate the enzyme through potential tuning. An already electrochemically activated enzyme sample was submitted to multiple cycling in a different potential range, where the anodic limits were higher, namely from −0.05 V to 0.192 to 0.542 V, in a solution with pH 7.6. The first scan, beginning at the open circuit potential, in the cathodic direction, results in a typical active Hase feature, where the H^+ reduction wave is well defined. On the second cycle, however, after the protein has been subjected to the higher potential scanning, is already possible to see the inactivation (Fig. 7A). The redox centers mentioned before could again be observed, and no response due to hydrogen reduction can be observed (inset of Fig. 7A). It should be noted that the redox processes observed on Fig. 4, resultant from the non-activated enzyme, and the ones observed on Fig. 7A (inset) present conformity between the potential values. The potential window is different in the two experiments, wider in Fig. 4 (cathodic limit −0.458 V) assay than in the inset of Fig. 7 (cathodic limit −0.258 V) which hinders the observation of process I. Process II_c presents a small 40 mV difference between the two assays, that may be due to the different inactivation methods.

In a wider potential window (Fig. 7B) is possible to observe, beside the redox signals mentioned before, the development of new signals

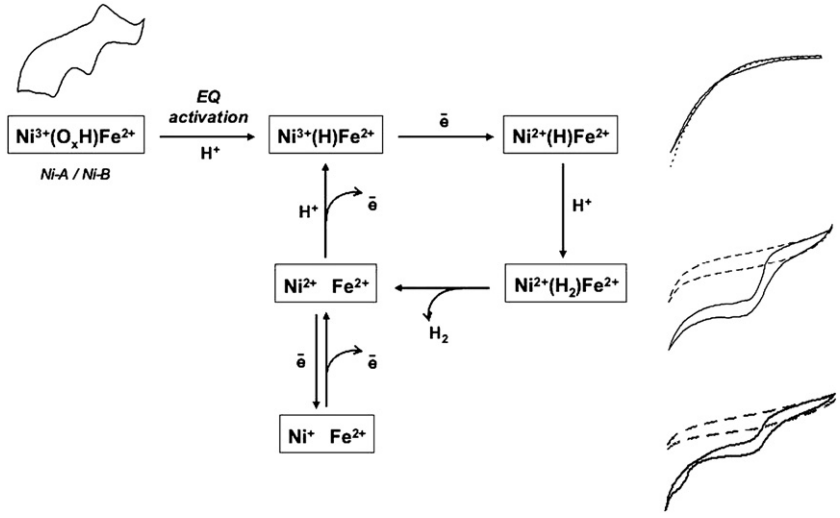

Fig. 8. Schematic representation of the proposed pathway for the Hase catalytic cycle under electrochemical control, with the correspondent voltammetric features.

at more anodic potential values, around 0.20 V. These last anodic processes may be associated with the formation of the Hase forms with the oxo/hydroxo bridge ligand. In fact the shape and potential domain of the above current peaks is quite similar to the ones observed by cyclic voltammetry for some nickel inorganic systems where the development of the metal hydroxides and other oxygenated species are described [32,33]. In the second cycle new cathodic processes, in two different regions, around −0.15 V, that are probably due to the reduction of the previous formed hydroxo/oxo species. These anodic features are better observed at higher pH, namely around 7, than in lower pH values (4–5), which seems consistent with the literature where the formation of these type of nickel oxo/hydroxides are reported in alkaline media [32].

After the described inactivation through the potential control, the electrochemical reactivation becomes very difficult. Indeed, application of the same electrochemical activation conditions as before the inactivation step did not result in the recovery of the initial current intensity for the hydrogen reduction (the maximum achieved for the reactivation was about 30% from the initial current intensity), which reflects the stability of the enzyme inactive forms and the poor reversibility of the reactions of the Hase with oxygen, as observed by other authors [17].

3.5. Electrochemical catalytic mechanism

Based on spectroscopic data [6,34] and theoretical calculations, as mentioned before, two different pathways have been proposed for the [NiFe]-Hase catalytic cycle, when the control is chemical by exposure to H_2, or electrochemical [4,6,34]. Putting together all the electrochemical observations made for active and inactive states of the enzyme, we accommodate the experimental results into the frame currently proposed for the Hase activation/inactivation process under electrochemical control (Fig. 8). In this representation we assume that either starting with Ni–A or Ni–B species we can activate the enzyme electrochemically in a step that involves the hydride bridge formation and the simultaneous reduction of Ni(III) to Ni(II). The catalytic cycle proceeds with the H_2 release and the Ni reoxidation and restoration of the hydride bridge. After the hydrogen molecule release the Ni (II) can be further reduced ton a Ni (I) state that does not seem, however, to be catalytically relevant.

4. Conclusions

In this work we were able to observe the direct electrochemistry of the *Dg* Hase, in bulk solution and immobilized with a membrane, in turnover and non-turnover conditions. For the first time the redox features of the enzyme metallic centers in non-catalytic conditions and without the addition of any of the known enzyme inhibitors were attained. Besides, we were able to tune the activation and inactivation of the Hase by dynamic potential control, where the formation of the hydride bridge was confirmed to be determinant.

Acknowledgments

CMC thanks the Fundação para a Ciência e Tecnologia, Portugal for funding (grant SFRH/BD/2917/2000).

References

[1] L. Pieulle, X. Morelli, P. Gallice, E. Lojou, P. Barbier, M. Czjzek, P. Bianco, F. Guerlesquin, E.C. Hatchikian, The type I/type II cytochrome c3 complex: an electron transfer link in the hydrogen-sulfate reduction pathway, J. Mol. Biol. 354 (2005) 73–90.
[2] I.B. Beech, J. Sunner, Biocorrosion: towards understanding interactions between biofilms and metals, Curr. Opin. Biotechnol. 15 (2004) 181–186.
[3] R. Mertens, A. Liese, Biotechnological applications of hydrogenases, Curr. Opin. Biotechnol. 15 (2004) 343–348.
[4] A. Pardo, A.L. De Lacey, V.M. Fernandez, H.J. Fan, Y. Fan, M.B. Hall, Density functional study of the catalytic cycle of nickel–iron [NiFe] hydrogenases and the involvement of high-spin nickel(II), J. Biol. Inorg. Chem. 11 (2006) 286–306.
[5] E.J. Lyon, S. Shima, G. Buurman, S. Chowdhuri, A. Batschauer, K. Steinbach, R.K. Thauer, UV-A/blue-light inactivation of the 'metal-free' hydrogenase (Hmd) from methanogenic archaea, Eur. J. Biochem. 271 (2004) 195–204.
[6] M. Teixeira, I. Moura, A.V. Xavier, J.J. Moura, J. Legall, D.V. Dervartanian, H.D. Peck Jr., B.H. Huynh, Redox intermediates of *Desulfovibrio gigas* [NiFe] hydrogenase generated under hydrogen. Mossbauer and EPR characterization of the metal centers, J. Biol. Chem. 264 (1989) 16435–16450.
[7] A.J. Pierik, W. Roseboom, R.P. Happe, K.A. Bagley, S.P. Albracht, Carbon monoxide and cyanide as intrinsic ligands to iron in the active site of [NiFe]-hydrogenases. NiFe(CN)2CO, Biology's way to activate H_2, J. Biol. Chem. 274 (1999) 3331–3337.
[8] M. Van Gastel, M. Stein, M. Brecht, O. Schroder, F. Lendzian, R. Bittl, H. Ogata, Y. Higuchi, W. Lubitz, A single-crystal ENDOR and density functional theory study of the oxidized states of the [NiFe] hydrogenase from *Desulfovibrio vulgaris* Miyazaki F, J. Biol. Inorg. Chem. 11 (2006) 41–51.
[9] A. Volbeda, L. Martin, C. Cavazza, M. Matho, B.W. Faber, W. Roseboom, S.P. Albracht, E. Garcin, M. Rousset, J.C. Fontecilla-Camps, Structural differences between the ready and unready oxidized states of [NiFe] hydrogenases, J. Biol. Inorg. Chem. 10 (2005) 239–249.
[10] A. Volbeda, J.C. Fontecilla-Camps, The active site and catalytic mechanism of NiFe hydrogenases, Dalton Trans. (2003) 4030–4038.
[11] M. Carepo, D.L. Tierney, C.D. Brondino, T.C. Yang, A. Pamplona, J. Telser, I. Moura, J.J. Moura, B.M. Hoffman, 17O ENDOR detection of a solvent-derived Ni–(OH(x))–Fe bridge that is lost upon activation of the hydrogenase from *Desulfovibrio gigas*, J. Am. Chem. Soc. 124 (2002) 281–286.
[12] H. Ogata, S. Hirota, A. Nakahara, H. Komori, N. Shibata, T. Kato, K. Kano, Y. Higuchi, Activation process of [NiFe] hydrogenase elucidated by high-resolution X-Ray analyses: conversion of the ready to the unready state, Structure (Camb.) 13 (2005) 1635–1642.
[13] A.K. Jones, S.E. Lamle, H.R. Pershad, K.A. Vincent, S.P. Albracht, F.A. Armstrong, Enzyme electrokinetics: electrochemical studies of the anaerobic interconversions between active and inactive states of *Allochromatium vinosum* [NiFe]-hydrogenase, J. Am. Chem. Soc. 125 (2003) 8505–8514.
[14] M.J. Maroney, P.A. Bryngelson, Spectroscopic and model studies of the Ni–Fe hydrogenase reaction mechanism, J. Biol. Inorg. Chem. 6 (2001) 453–459.
[15] A.L. De Lacey, J. Moiroux, C. Bourdillon, Simple formal kinetics for the reversible uptake of molecular hydrogen by [Ni–Fe] hydrogenase from *Desulfovibrio gigas*, Eur. J. Biochem. 267 (2000) 6560–6570.
[16] Y. Montet, P. Amara, A. Volbeda, X. Vernede, E.C. Hatchikian, M.J. Field, M. Frey, J.C. Fontecilla-Camps, Gas access to the active site of Ni–Fe hydrogenases probed by X-ray crystallography and molecular dynamics, Nat. Struct. Biol. 4 (1997) 523–526.
[17] K.A. Vincent, J.A. Cracknell, A. Parkin, F.A. Armstrong, Hydrogen cycling by enzymes: electrocatalysis and implications for future energy technology, Dalton Trans. (2005) 3397–3403.
[18] E. Lojou, P. Bianco, Membrane electrodes can modulate the electrochemical response of redox proteins — direct electrochemistry of cytochrome c, J. Electroanal. Chem. 485 (2000) 71–80.
[19] S.V. Morozov, E.E. Karyakina, N.A. Zorin, S.D. Varfolomeyev, S. Cosnier, A.A. Karyakin, Direct and electrically wired bioelectrocatalysis by hydrogenase from *Thiocapsa roseopersicina*, Bioelectrochemistry 55 (2002) 169–171.
[20] H. Tatsumi, K. Takagi, M. Fujita, K. Kano, T. Ikeda, Electrochemical study of reversible hydrogenase reaction of *Desulfovibrio vulgaris* cells with methyl viologen as an electron carrier, Anal. Chem. 71 (1999) 1753–1759.
[21] H.R. Pershad, J.L. Duff, H.A. Heering, E.C. Duin, S.P. Albracht, F.A. Armstrong, Catalytic electron transport in Chromatium vinosum [NiFe]-hydrogenase: application of voltammetry in detecting redox-active centers and establishing that hydrogen oxidation is very fast even at potentials close to the reversible H+/H_2 value, Biochemistry 38 (1999) 8992–8999.
[22] J. Legall, P.O. Ljungdahl, I. Moura, H.D. Peck Jr., A.V. Xavier, J.J. Moura, M. Teixera, B.H. Huynh, D.V. Dervartanian, The presence of redox-sensitive nickel in the periplasmic hydrogenase from *Desulfovibrio gigas*, Biochem. Biophys. Res. Commun. 106 (1982) 610–616.
[23] D.M. Soares, Hydride effect on the kinetics of the hydrogen evolution reaction on nickel cathodes in alkaline media, J. Electrochem. Soc. 139 (1992) 98–105.
[24] V. Vivier, C. Cachet-Vivier, J.Y. Nedelec, L.T. Yu, J.M. Joubert, A. Percheron-Guegan, Electrochemical study of LaNi3.55Mn0.4Al0.3Co0.75 by cavity microelectrode in 7 mol 1(−1) KOH solution, J. Power Sources 124 (2003) 564–571.
[25] C. Leger, A.K. Jones, W. Roseboom, S.P. Albracht, F.A. Armstrong, Enzyme electrokinetics: hydrogen evolution and oxidation by *Allochromatium vinosum* [NiFe]-hydrogenase, Biochemistry 41 (2002) 15736–15746.
[26] M. Teixeira, I. Moura, A.V. Xavier, B.H. Huynh, D.V. Dervartanian, H.D. Peck Jr., J. Legall, J.J. Moura, Electron paramagnetic resonance studies on the mechanism of activation and the catalytic cycle of the nickel-containing hydrogenase from *Desulfovibrio gigas*, J. Biol. Chem. 260 (1985) 8942–8950.
[27] K. Chen, C.A. Bonagura, G.J. Tilley, J.P. Mcevoy, Y.S. Jung, F.A. Armstrong, C.D. Stout, B.K. Burgess, Crystal structures of ferredoxin variants exhibiting large changes in [Fe-S] reduction potential, Nat. Struct. Biol. 9 (2002) 188–192.
[28] G.J. Tilley, R. Camba, B.K. Burgess, F.A. Armstrong, Influence of electrochemical properties in determining the sensitivity of [4Fe-4S] clusters in proteins to oxidative damage, Biochem. J. 360 (2001) 717–726.
[29] S. Foerster, M. Stein, M. Brecht, H. Ogata, Y. Higuchi, W. Lubitz, Single crystal EPR studies of the reduced active site of [NiFe] hydrogenase from *Desulfovibrio vulgaris* Miyazaki F, J. Am. Chem. Soc. 125 (2003) 83–93.
[30] M. Stein, E. Van Lenthe, E.J. Baerends, W. Lubitz, Relativistic DFT calculations of the paramagnetic intermediates of [NiFe] hydrogenase. Implications for the enzymatic mechanism, J. Am. Chem. Soc. 123 (2001) 5839–5840.

[31] T. Lissolo, S. Pulvin, D. Thomas, Reactivation of the Hydrogenase from *Desulfovibrio-gigas* by hydrogen — Influence of redox potential, J. Biol. Chem. 259 (1984) 1725–1729.
[32] A.M. Fundo and L.M. Abrantes, The electrocatalytic behaviour of electroless Ni–P alloys, Journal of Electroanalytical Chemistry In Press, Corrected Proof.
[33] J.R.C. Salgado, M.H.S. Andrade, J.C.P. Silva, J. Tonholo, A voltammetric study of alpha- and beta-hydroxides over nickel alloys, Electrochim. Acta 47 (2002) 1997–2004.
[34] A. Volbeda, J.C. Fontecilla-Camps, Structure–function relationships of nickel–iron sites in hydrogenase and a comparison with the active sites of other nickel–iron enzymes, Coord. Chem. Rev. 249 (2005) 1609–1619.